

RESEARCH ARTICLE

Chimera states in Gaussian coupled map lattices

Xiao-Wen Li[†], Ran Bi, Yue-Xiang Sun, Shuo Zhang, Qian-Qian Song

Department of Physics, Beijing Normal University, Beijing 100875, China

Corresponding author. E-mail: [†]xwli@bnu.edu.cn

Received May 19, 2017; accepted September 12, 2017

We study chimera states in one-dimensional and two-dimensional Gaussian coupled map lattices through simulations and experiments. Similar to the case of global coupling oscillators, individual lattices can be regarded as being controlled by a common mean field. A space-dependent order parameter is derived from a self-consistency condition in order to represent the collective state.

Keywords chimera state, coupled map lattices, nonlocal coupling

PACS numbers 05.45.Xt, 82.40.Ck, 89.75.Kd, 85.60.-q

1 Introduction

In 2002, Kuramoto and Battogtokh found that an array of identical oscillators with nonlocal coupling could be split into two domains with certain parameters and initial conditions: one composed of coherent oscillators that are mutually synchronized with a unique frequency and the other composed of incoherent oscillators that desynchronized with distributed frequencies [1]. In this regard, they developed the mean field theory, which worked very well for globally coupled systems, in simulating the collective dynamics of nonlocal coupled oscillators. This phenomenon was called the “Chimera state” which refers to anything that is composed of incompatible parts. An exact solution for the chimera state was obtained by introducing a new complex parameter and studying a one-dimensional ring of phase oscillators that were coupled nonlocally by a cosine kernel [2, 3]. The dynamics and bifurcations of the chimera state were clarified by studying two interacting populations of phase oscillators [4–6]. In two-dimensional spatially extended systems, the chimera state manifests as rotating spiral waves with a phase-randomized core [7]. An analytical description of such a spiral wave chimera was provided in addition. Its rotational speed and the size of its incoherent core can be calculated by using perturbation theory [8]. Clustered chimera states were also found in a ring of identical phase oscillators that were coupled in a time-delayed and spatially nonlocal fashion. The existence of time-delay induced phase clustering was verified through the solutions of a self-consistency equation for the mean field [9].

Not only nonlocal coupling identical phase oscillators, but also non-phase models, such as neurons [10] and chaotic maps, can yield chimera states with certain parameters and initial conditions. A nonlocal coupling network of chaotic iterated maps was experimentally confirmed to contain coexisting spatial domains of coherence and incoherence [11]. In this paper, we present chimera states in one-dimensional or two-dimensional Gaussian coupled map lattices. Similar to the mean field theory, which has been successfully applied to global coupling oscillators, an order parameter is defined to represent the collective state. In contrast to the study in Ref. [11], we apply Gaussian coupling, which represents the true distribution of a laser beam. We define an order parameter for a coupled map system, which can be used as an observable value for the system when we attempt to control the chimera state.

2 Experimental setup and model

Our experimental system is comprised of a liquid-crystal spatial light modulator (SLM), lens, quarter-wave plate, polarizing beam splitter, CCD camera, computer, and laser (635 nm). Figure 1 presents the experimental setup for our system.

Collimated 635-nm light from the laser passes through a polarizing beam splitter and quarter-wave plate, which is oriented 45° from the long axis of the SLM. The SLM reflects the light with a relative phase shift between the fast and slow axes. The reflected light passes through the quarter-wave plate and beam splitter again before it illuminates the camera. We use the computer-controlled

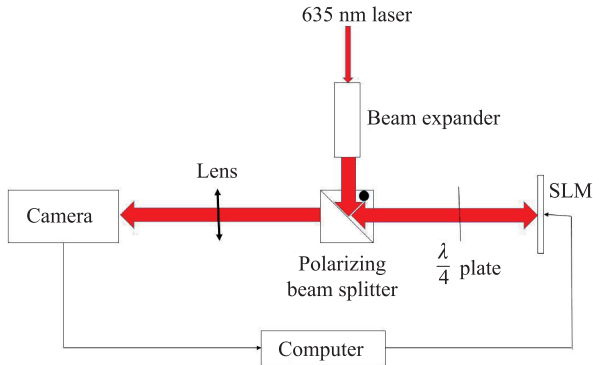


Fig. 1 Experimental setup.

SLM to apply arbitrary and spatially-dependent phase modulation to the optical wavefront by using a birefringent liquid crystal suspended between an array of reflective electrodes and a transparent cover glass. Each of the electrodes acts as an independent pixel that can impose an arbitrary phase shift ranging from 0 to 2π between the two polarization components of the incoming light by applying an electric field in order to reorient the liquid crystal. The polarization optics create a nonlinear relationship between the phase shift φ applied by the SLM and the intensity of the light incident on the camera [11, 12],

$$I = \frac{I_0}{2}(1 + \cos \varphi). \quad (1)$$

We use the light intensity I as a feedback signal in order to communicate with the SLM and choose an appropriate lookup table such that the phase shift φ is proportional to the light intensity:

$$\varphi = 2\pi I. \quad (2)$$

The current light intensity has a nonlinear relationship with the light intensity at the previous moment, which can be expressed as follows:

$$I_{n+1} = \frac{I_0}{2}[1 + \cos(2\pi I_n)]. \quad (3)$$

In this setup, we use a lens to project every SLM pixel onto a single camera pixel. The SLM we used has 512×512 pixels. We construct a network of iterative maps by using a computer to link the camera to the SLM. Each pixel in the SLM or camera corresponds to a node in the network of coupled maps. The dimensions of such a CML can be up to 512×512 . Feedback is achieved by iteratively updating the phase applied to the SLM by each pixel, which depends on the light intensity measured by the camera.

In this paper, we use one-dimensional and two-

dimensional Gaussian coupled map lattices as follows:

$$\phi_i^{n+1} = 2\pi a \left\{ I(\phi_i^n) + \frac{1}{2R} \sum_{k=-R}^R \varepsilon [I(\phi_{i+k}^n) - I(\phi_i^n)] \right\} \quad (4)$$

$$\phi_{i,j}^{n+1} = 2\pi a \left\{ I(\phi_{i,j}^n) + \frac{1}{4R^2} \sum_{k,l=-R}^R \varepsilon [I(\phi_{i+k,j+l}^n) - I(\phi_{i,j}^n)] \right\} \quad (5)$$

Here, $i, j = 0, 1, 2, \dots, N - 1$. n denotes the discrete time. Each element is coupled diffusively to all the elements within a distance R on either side and ε describes the Gaussian distribution of coupling. $\varepsilon = a_0 \exp(-qd^2)$. $q = \frac{9}{2R^2}$ guarantees that R is equal to three standard deviations. a_0 represents the strength of the Gaussian coupling. $d = \min(|k|, N - |k|)$ for one dimension and $d = \sqrt{d_1^2 + d_2^2}$ where $d_1 = \min(|k|, N - |k|)$. $d_2 = \min(|l|, N - |l|)$ for two dimensions.

3 Chimera states

Figure 2 characterizes the dependence of the dynamics of the one-dimensional system on the coupling strength a_0 and coupling range $r = R/N$ by plotting snapshots of the phase. The phase is incoherent when the coupling strength a_0 or couple range r is small, as shown in Figs. 2(a), (b), (d), and (g). When the system couples with medium strength and distance, it is divided into two groups. One is coherent while the other is incoherent, as shown in Figs. 2(c), (e), (f), and (h). When

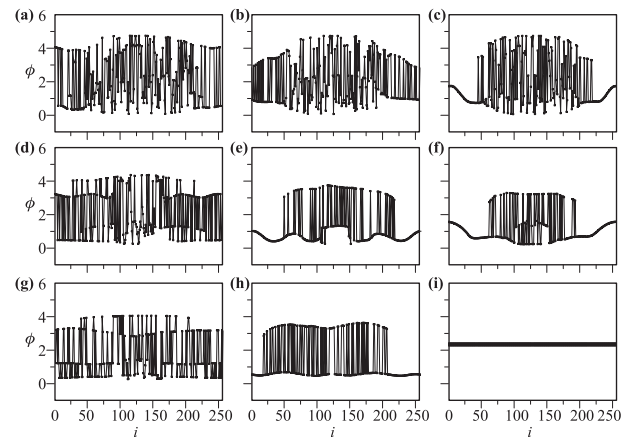


Fig. 2 Snapshot of the phase with different coupling strengths and ranges. $r = R/N$ represents the coupling range. R is the coupling distance. a_0 represents the strength of the Gaussian coupling $\varepsilon = a_0 \exp(-qd^2)$. (a) $r = 0.230$, $a_0 = 0.50$; (b) $r = 0.230$, $a_0 = 0.85$; (c) $r = 0.230$, $a_0 = 1.00$; (d) $r = 0.414$, $a_0 = 0.50$; (e) $r = 0.414$, $a_0 = 0.85$; (f) $r = 0.414$, $a_0 = 1.00$; (g) $r = 0.450$, $a_0 = 0.50$; (h) $r = 0.450$, $a_0 = 0.85$; (i) $r = 0.450$, $a_0 = 1.00$.

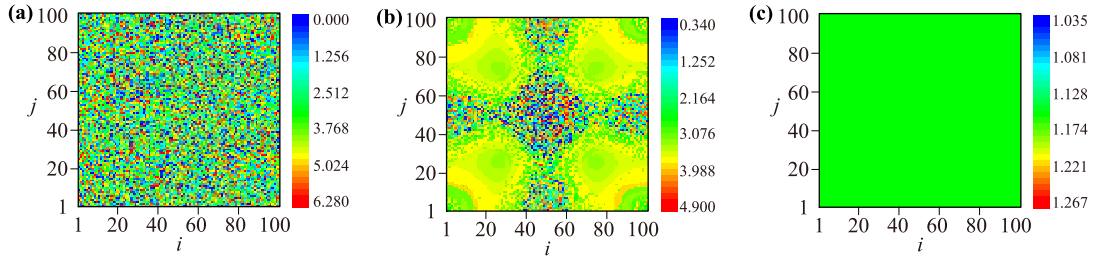


Fig. 3 Snapshot of the phase in the two-dimensional system. $r = R/N$ represents the coupling range. R is the coupling distance. a_0 represents the strength of the Gaussian coupling $\varepsilon = a_0 \exp(-qd^2)$. (a) $r = 0.25$, $a_0 = 0.60$; (b) $r = 0.41$, $a_0 = 0.65$; (c) $r = 0.47$, $a_0 = 1.50$.

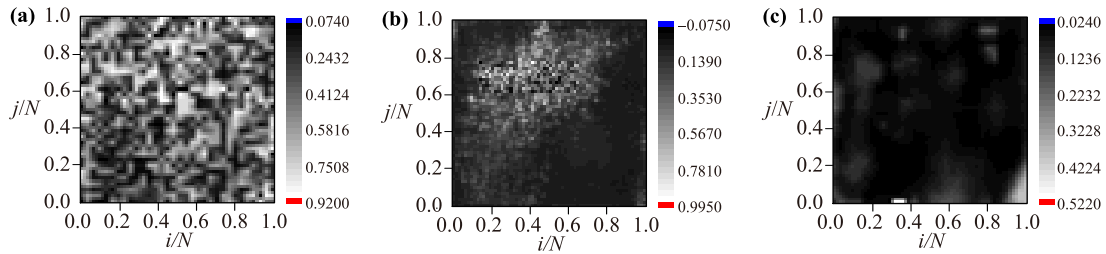


Fig. 4 Experimental results for the phase of the two-dimensional system. $r = R/N$ represents the coupling range. R is the coupling distance. a_0 represents the strength of the Gaussian coupling $\varepsilon = a_0 \exp(-qd^2)$. (a) $r = 0.25$, $a_0 = 0.60$; (b) $r = 0.41$, $a_0 = 0.65$; (c) $r = 0.49$, $a_0 = 1.50$.

the coupling strength and distance become sufficiently large, the system reaches chaotic synchrony, as shown in Fig. 2(i).

The two-dimensional system exhibits similar phenomena, as shown in Fig. 3. As the coupling distance and strength increase, the system first becomes chaotic, as shown in Fig. 3(a). Then it enters the chimera state, as shown in Fig. 3(b). The spatial distribution of this two-dimensional system is divided into two domains: one coherent and phase-locked, and the other incoherent and desynchronized. In other words, the phase distribution is continuous in the region near the four corners and chaotic in the middle. Finally, it reaches chaotic synchrony, as shown in Fig. 3(c).

Figure 4 presents our experimental results. Using different parameters, the system exhibits the chaotic state (a), chimera state (b), and synchronously chaotic state (c).

As a generalization of the theory of synchronization transitions in globally coupled phase oscillators with frequency distributions, a complex order parameter with modulus A and phase Θ is introduced into the continuous nonlocal coupled phase oscillators [1]:

$$A(x, t) \exp[i\Theta(x, t)] = \int dx' G(x - x') \exp[i\Phi(x')]. \quad (6)$$

where $G(x - x')$ represents the coupled equations. Thus, the system is transformed into an assembly of independent oscillators under the control of a common force field

represented by A and Θ . Similarly, we define an order parameter for the coupled map lattices system:

$$A_j^n \exp[i\Theta_j^n] = \frac{a_0}{2R} \sum_{k=-R}^R \exp\left[-\frac{9}{2R^2}(j-k)^2\right] \exp[i\phi_k^n]. \quad (7)$$

The spatial profiles of A_j and Θ_j are presented in Fig. 5. We can see that the force mean-field amplitude is stronger in the coherent domain and weaker in the incoherent domain. The order parameter amplitude reaches its maximum at the center of the coherent domain. The dynamics of the system can be summarized as follows: The system is divided into two subgroups of lattices. In the first group, the force amplitude is large enough for the lattices to be entrained, meaning they are coherent. In the second group, the force amplitude is too weak for entrainment, meaning the lattices are desynchronized. The threshold of force amplitude for entraining the lattices increases as the coupling strength a_0 increases, as indicated by A_c in Fig. 5. Table 1 reveals that the critical order parameter increases as the coupling strength increases with a set r . Table 2 reveals that the order parameter also increases with an increasing r while a_0 is set. Therefore, the order parameter reflects the instantaneous spatial distribution of the system to a certain degree, and the critical order parameter is an important physical quantity for describing the coherent and incoherent spatial distributions in the chimera state.

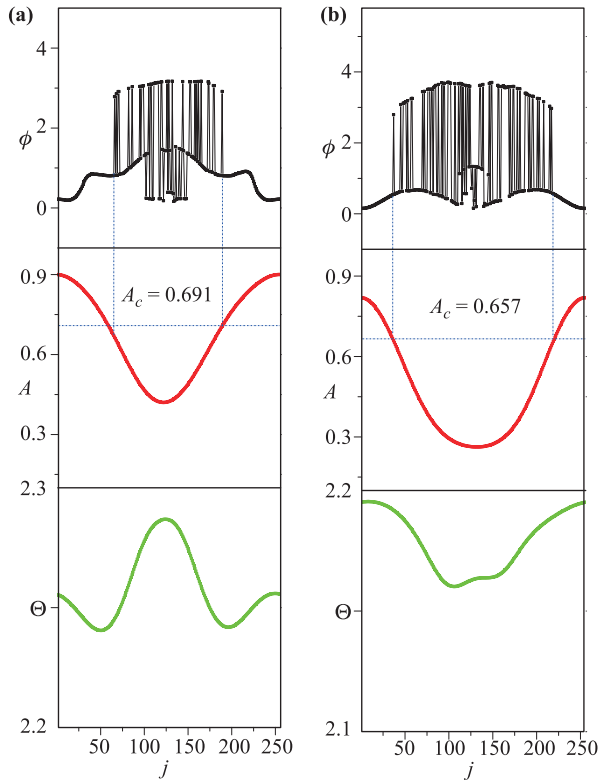


Fig. 5 Order parameter. $r = R/N$ represents the coupling range. R is the coupling distance. a_0 represents the strength of the Gaussian coupling $\varepsilon = a_0 \exp(-qd^2)$. **(a)** $r = 0.414$, $a_0 = 1.00$; **(b)** $r = 0.414$, $a_0 = 0.85$.

Table 1 $r = 0.41$. The critical order parameter A_c with varied coupling strength a_0 .

a_0	A_c
0.50	0.2292
0.52	0.2969
0.55	0.3406
0.58	0.4056
0.60	0.4631
0.62	0.5108
0.65	0.5202

Table 2 $a_0 = 0.65$. The critical order parameter A_c with varied coupling range r .

r	A_c
0.40	0.4335
0.41	0.5202
0.42	0.5914
0.43	0.6942

4 Discussion

We studied chimera states in Gaussian coupled map lattices. Similar to the case of global coupling oscillators,

the individual lattices can be regarded as being controlled by a common mean field. In both systems, a suitably defined order parameter representing the collective state is derived from a condition of self-consistency, which must exist between the collective dynamics and the dynamics of the individual lattices. Because the order parameter is space-dependent and its amplitude A reaches a maximum at the center of the coherent domain, we can consider A as an observable value for the system. This will allow us to develop a control scheme to dynamically modulate the position of the coherent portion of a chimera state in the future.

References

1. Y. Kuramoto and D. Battogtokh, Coexistence of coherence and incoherence in nonlocally coupled phase oscillators, *Nonlin. Phenom. Complex Syst.* 5(4), 380 (2002)
2. D. M. Abrams and S. H. Strogatz, Chimera states for coupled oscillators, *Phys. Rev. Lett.* 93(17), 174102 (2004)
3. D. M. Abrams and S. H. Strogatz, Chimera states in a ring of nonlocally coupled oscillators, *Int. J. Bifurcat. Chaos* 16(01), 21 (2006)
4. D. M. Abrams, R. Mirollo, S. H. Strogatz, and D. A. Wiley, Solvable model for chimera states of coupled oscillators, *Phys. Rev. Lett.* 101(8), 084103 (2008)
5. A. Pikovsky and M. Rosenblum, Partially integrable dynamics of hierarchical populations of coupled oscillators, *Phys. Rev. Lett.* 101(26), 264103 (2008)
6. C. R. Laing, Chimera states in heterogeneous networks, *Chaos* 19(1), 013113 (2009)
7. S. i. Shima and Y. Kuramoto, Rotating spiral waves with phase-randomized core in nonlocally coupled oscillators, *Phys. Rev. E* 69(3), 036213 (2004)
8. E. A. Martens, C. R. Laing, and S. H. Strogatz, Solvable model of spiral wave chimeras, *Phys. Rev. Lett.* 104(4), 044101 (2010)
9. G. C. Sethia, A. Sen, and F. M. Atay, Clustered chimera states in delay-coupled oscillator systems, *Phys. Rev. Lett.* 100(14), 144102 (2008)
10. C. H. Tian, X. Y. Zhang, Z. H. Wang, and Z. H. Liu, Diversity of chimera-like patterns from a model of 2D arrays of neurons with nonlocal coupling, *Front. Phys.* 12(3), 128904 (2017)
11. A. M. Hagerstrom, T. E. Murphy, R. Roy, P. Hövel, I. Omelchenko, and E. Schöll, Experimental observation of chimeras in coupled-map lattices, *Nat. Phys.* 8(9), 658 (2012)
12. Y. H. Ma, L.Q. Huang, C. M. Sun, and X. W. Li, Experimental system of coupled map lattices, *Front. Phys.* 10(3), 100504 (2015)